

# S-wave Pairing of $\Lambda$ Hyperons in Dense Matter

Shmuel Balberg<sup>1</sup> and Nir Barnea<sup>1,2</sup>

<sup>1</sup> *The Racah Institute of Physics, The Hebrew University, Jerusalem 91904, Israel*

<sup>2</sup> *ECT\*, European Centre for Theoretical Studies in Nuclear Physics and Related Areas,  
Strada delle Tabarelle 286, I-38050 Villazzano (Trento), Italy*

(April 1, 2018)

## Abstract

In this work we calculate the  $^1S_0$  gap energies of  $\Lambda$  hyperons in neutron star matter. The calculation is based on a solution of the BCS gap equation for an effective  $G$ -matrix parameterization of the  $\Lambda$ - $\Lambda$  interaction with a nuclear matter background, presented recently by Lansky and Yamamoto. We find that a gap energy of a few tenths of MeV is expected for  $\Lambda$  Fermi momenta up to about  $1.3 \text{ fm}^{-1}$ . Implications for neutron star matter are examined, and suggest the existence of a  $\Lambda$   $^1S_0$  superfluid between the threshold baryon density for  $\Lambda$  formation and the baryon density where the  $\Lambda$  fraction reaches 15–20%.

*PACS:* 26.60.+c, 97.60.Jd, 14.20.Jn

## I. INTRODUCTION

The theory of neutron star structure directly relates global properties of these stars to various aspects of many-baryon physics. One fundamental issue is whether pairing forces among the baryons can give rise to baryon superfluids in the inner crust and quantum cores of neutron stars. While nucleon pairing in neutron stars has received much attention, quantitative estimates of pairing of other baryon species has not been performed to date, due to lack of relevant experimental data. In this work we use some recent analysis of hypernuclei to make a first attempt at determining superfluid gaps for  $\Lambda$  hyperons in neutron star matter.

Since first suggested by Migdal [1], nucleon pairing in nuclear matter has been the subject of many studies. Both former [2,3] and recent [4-8] works typically find  $^1S_0$  neutron pairing for neutron matter density,  $\rho_n$ , in the range of  $0.1\rho_0 \leq \rho_n \leq 0.5\rho_0$ , where  $\rho_0 \approx 0.16 \text{ fm}^{-3}$  is the nuclear saturation density. At higher densities, the  $^1S_0$  interaction turns repulsive, and pairing is possible through higher order interactions, mainly  $^3P_2$  [9,10]. The energy gap found for the  $^1S_0$  neutron superfluid is typically of the order of a few MeV, although recent works [6,7] suggest that quasi-particle correlations could lower the energy to about 1 MeV. Estimates of the  $^3P_2$  gap are typically of the order of a few tenths of a MeV. It should be noted that published results for the pairing energy gaps differ by as much as a factor of three. The difficulty in obtaining accurate results is mainly due to the problem of consistently including background medium effects. Uncertainties in the two-body interactions pose an additional problem.

As the temperature of a neutron star is expected to drop below 0.1 MeV ( $\sim 10^9$  K) within about one day from its birth, it is widely accepted that nucleon superfluids exist in different regions of the star. The qualitative picture of a neutron star includes a  $^1S_0$  neutron superfluid in its inner crust (along with neutron rich nuclei), and a  $^3P_2$  neutron superfluid in the quantum liquid core. The protons in the core, having a partial density of about 10% of the neutrons, are also expected to be in a  $^1S_0$  superfluid, with an energy gap of about 1 MeV. [7,8].

Baryon superfluids are expected to have a number of important consequences on neutron star physics including several observational effects, such as pulsar glitch phenomena and cooling rates. The crustal neutron superfluid is expected to play an incisive role in the driving mechanism of pulsar glitches, due to pinning of the neutron superfluid to the nuclei [11]. Core nucleon superfluids may significantly suppress cooling rates that rely on neutrino emission, by reducing the available phase space in the final state [12,13].

In this work we focus on the inner core of neutron stars, where baryon species other than nucleons are expected to appear. It is widely accepted [14-18] that hyperons begin to accumulate at a density of about  $2\rho_0$ , and at a density of  $3\rho_0$  the hyperon fraction is already about 0.2. These results are a direct consequence of using modern estimates of the interactions of hyperons in nuclear matter, derived from hypernuclei experiments. The presence of hyperons has been shown to be of considerable importance in neutron star cooling rates due to their potential to participate in the efficient direct Urca processes. While hyperon direct Urca is found to be small compared to the nucleon direct Urca when nucleons are non-superfluid, hyperon direct Urca becomes the predominating coolant if the nucleons form superfluid pairs [19]. It is noteworthy that the direct Urca mechanism can proceed through hyperon processes for almost any hyperon fraction, while the nucleon direct Urca requires a proton fraction of at least 0.11–0.15 [20,21]. In fact, some studies have found that hyperon direct Urca cooling is too rapid to be consistent with observed surface temperatures of pulsars [19,22,23]. However, if hyperons also couple to a superfluid state, as expected for the nucleons, hyperon direct Urca will also be suppressed, and a large hyperon fraction could be easier to coincide with observed cooling rates.

Hyperon pairing has not been studied previously, as the basic obstacles relevant to nucleonic pairing are pronounced for hyperons. However, a few measured events in KEK experiments [24] attributed to doubly-strange  $\Lambda\Lambda$  hypernuclei, do offer indication with regard to the  $\Lambda-\Lambda$  interaction with a background nuclear matter medium. In a recent work Lanskoj and Yamamoto [25] formulated a G-matrix parameterization for the  $\Lambda-\Lambda$  interaction, based on Nijmegen OBE models. This G-matrix includes a dependence on the density of the nuclear matter medium, and reproduces the experimental results of the  $\Lambda\Lambda$  hypernuclei.

In this work we aim to employ this formulation to estimate  $\Lambda\Lambda$  pairing energies in dense matter. We briefly review in Sec. II the formalism leading to the gap equation in the  $^1S_0$  channel. The properties of the effective potential used in this work are introduced in Sec. III. Sec. IV presents our results for the superfluid gap of  $\Lambda\Lambda$  S-wave pairing in nuclear matter. Implications for neutron stars are discussed in Sec. V. Sec. VI contains our conclusions and some out-looks regarding hyperon pairing.

## II. THE GAP EQUATION

The BCS theory [26] predicts a transition to the superfluid phase when correlations leading to Cooper  $^1S_0$  pairs give rise to excessive binding energy, which overcompensates the increase of energy due to the depopulation of the Fermi sea. The appropriate equations have been formulated in many works (see, for example, in refs. [4,7,8]), and for completeness we

review below the main results. We note in passing that variation of definitions may lead to differences in the numerical coefficients with respect to other works.

The binding energy of a pair with momenta  $(\mathbf{k}, -\mathbf{k})$  is found through a nonzero solution to the gap equation

$$\Delta_k = -\frac{1}{2} \sum_{k'} V_{kk'} \frac{\Delta_{k'}}{(\xi_{k'}^2 + \Delta_{k'}^2)^{\frac{1}{2}}} \quad , \quad (1)$$

where  $\Delta_k$  is known as the gap function. The potential  $V_{kk'}$  is defined through the matrix element of the  $^1S_0$  component of the interaction, and  $\xi_k$  corresponds to the single particle energy,  $\varepsilon_k$ , when measured with respect to the Fermi surface.

Going over to formal integration, the potential term is replaced by the potential matrix element:  $\langle \mathbf{k} \uparrow -\mathbf{k} \downarrow | V | \mathbf{k}' \uparrow -\mathbf{k}' \downarrow \rangle$ . In the special case of the  $^1S_0$  channel the matrix element is independent of the orientation of  $\mathbf{k}$  and  $\mathbf{k}'$ . For a two-particle central potential,  $V(r)$ , the matrix element can be reduced to the form:

$$V_{kk'} \equiv \langle k | V(^1S_0) | k' \rangle = 4\pi \int_0^\infty r^2 dr j_0(kr) V(r) j_0(k'r) \quad (2)$$

For convenience unit normalization volume is taken for the plane wave single particle wave functions; summation over spatial and spin exchange terms is implied.

The integral form of the gap equation is thus:

$$\begin{aligned} \Delta_k &= -\frac{1}{2} \frac{1}{(2\pi)^3} \int 4\pi k'^2 dk' V_{kk'} \frac{\Delta_{k'}}{(\xi_{k'}^2 + \Delta_{k'}^2)^{\frac{1}{2}}} = \\ &= -\frac{1}{\pi} \int k'^2 dk' \frac{\Delta_{k'}}{(\xi_{k'}^2 + \Delta_{k'}^2)^{\frac{1}{2}}} \int r^2 dr j_0(kr) V(r) j_0(k'r) \quad . \end{aligned} \quad (3)$$

In this work we use the common “decoupling approximation”, where the Fermi surface is taken to be sharp even in the presence of the pairing correlations. The functions  $\xi_k$  are then simply given by

$$\xi_k = \varepsilon_k - \varepsilon_{k_F} \quad , \quad (4)$$

where we calculated the single particle energies with first order Hartree-Fock corrections [27].

The effect of the pairing potential on the single particle energies is often characterized by an effective particle mass,  $M^*$ , which is typically lower than the initial (bare) mass by several percent. This mass can be estimated through the effective mass approximation:

$$M^* = \left( \frac{1}{\hbar^2 k_F} \frac{d\varepsilon_k}{dk} \Big|_{k=k_F} \right)^{-1} \quad , \quad (5)$$

which is usually found to be good up to a few percent [7].

Note that this effective mass differs from the bulk effective mass, found in field theories due to the meson scalar field, also typically lower than the bare mass [17]. A consistent theory thus requires an appropriate “true” initial mass, which includes medium effects through both the  $\Lambda-\Lambda$  and  $\Lambda$ -nucleon interactions. However, in the present work we invoke a non-relativistic approach, which has no means to consistently combine effective bulk masses, and correspondingly set the initial mass to be equal to the bare mass, i.e.,  $M_\Lambda = 1115.6$  MeV (some justification for this may also be found in uncertainties regarding values of effective masses at the Fermi surface [28]). The sensitivity of  $\Lambda$  pairing to this assumption is examined below.

### III. THE $\Lambda - \Lambda$ POTENTIAL

In this work we approximate the  $^1S_0$  component of the  $\Lambda\Lambda$  interaction through a Brueckner  $G$ -matrix potential. We use the very recent  $G$ -matrix parameterization of Lansky and Yamamoto [25] derived from the Nijmegen OBE potentials for a  $\Lambda\Lambda$  pair in nuclear matter. Their evaluation of the  $\Lambda\Lambda$  interaction is based on measurements of doubly strange hypernuclei observed in experiments [24]. Analysis of these experiments has suggested both the existence of an attractive component in the  $\Lambda - \Lambda$  interaction and the dependence of this interaction on the properties of the core nucleus [30]. The strength of the interaction is derived from the bond energy of the  $\Lambda\Lambda$  pair, defined as  $\Delta B_{\Lambda\Lambda} = B_{\Lambda\Lambda} - 2B_\Lambda$ . Here  $B_{\Lambda\Lambda}$  is the separation energy of two  $\Lambda$ 's from the nucleus and  $B_\Lambda$  is the separation energy of a single  $\Lambda$  from the same nucleus.

The dependence of the interaction on the nuclear matter density is represented in Ref. [25] by a three-range Gaussian form:

$$V_{\Lambda\Lambda}(r) = \sum_{i=1}^3 (a_i + b_i k_F(n) + c_i k_F^2(n)) \exp(-r^2/\beta_i^2) \quad , \quad (6)$$

where  $k_F(n)$  is the nucleon Fermi momentum. Assuming symmetric nuclear matter (as is the case for light hypernuclei),  $k_F$  is related to the nuclear density  $\rho_N$  by  $k_F = (3\pi^2 \frac{1}{2} \rho_N)^{\frac{1}{3}}$ . Since the  $\Lambda$  is an isospin singlet, it also seems safe to apply equation (6) to non-symmetric nuclear matter of density  $\rho_N$ .

The ranges  $\beta_i$  and the strength parameters  $a_i, b_i, c_i$  are taken from model ND of [25] and are listed in table I. This model successfully reproduces the experimental result of  $\Delta B_{\Lambda\Lambda} = 4.9 \pm 0.7$  MeV of  ${}^{13}_{\Lambda\Lambda}B$  [24].

The radial dependence of the  $\Lambda$ – $\Lambda$  interaction is demonstrated in Fig. 1 which shows  $V_{\Lambda\Lambda}(r)$  for nuclear matter densities of  $\rho_N/\rho_0 = 1$ ,  $\rho_N/\rho_0 = 2.5$  and  $\rho_N/\rho_0 = 5$ . At short distances the interaction is always repulsive, reflecting the core repulsion of the bare interaction (we note that  $G$ -matrix approximations typically yield soft cores [6] which substitute the need for short range cut-off necessary in other interaction models). At intermediate distances the  $^1S_0$  yields an attractive force of several tens of MeV’s, which is strong enough to yield the pairing of the superfluid state.

As can be seen in Fig. 1, the dependence of the interaction on the nuclear matter density is rather weak. This implies that the existence of  $^1S_0$  pairing should have only a moderate dependence on the density of the nuclear matter medium. We note, however, that the magnitude of the interaction tends to grow larger for a larger background density.

It must be noted that the  $G$ -matrix parameterization is fitted to match experimental results for different nuclei, and is thus likely to be valid for a nuclear matter background with a density of  $\rho_N \approx \rho_0$ . In the following analysis we assume that the  $G$ -matrix is valid for higher densities as well. Clearly this is a somewhat crude assumption, especially since the  $G$ -matrix does not incorporate any relativistic effects which could be significant at densities relevant to neutron star cores ( $\rho \geq 2\rho_0$ ). Hence, the results derived below must be viewed as preliminary estimates. More founded results must await better established  $\Lambda\Lambda$  potentials in high density nuclear matter.

#### IV. RESULTS FOR $\Lambda$ PAIRING IN DENSE MATTER

Using the  $\Lambda\Lambda$  potential described in the previous Section, we have solved the gap equation, Eq. (3), for  $\Lambda$  hyperons in a nuclear matter background. The solution is found by iterations, when the integration is performed with a few hundred integration points, exponentially spaced around  $k_F(\Lambda)$ . The exponential spacing is required since the integrand in Eq. (3) is sharply peaked at the Fermi momentum. This behavior is demonstrated in Fig. 2 which shows the integrand for a  $\Lambda$  Fermi momenta of  $k_F(\Lambda) = 1.0 \text{ fm}^{-1}$  and nuclear matter densities of  $\rho_N = 2.5\rho_0$  and  $\rho_N = 5.0\rho_0$ . Fig. 2 also indicates the need for a large cutoff momenta in the calculation of the gap function in Eq. (3).

Solution of the gap equations gives the gap function  $\Delta_k$  for any combination of values for the nuclear matter background density and the  $\Lambda$  Fermi momenta. Fig. 3 shows the gap function for the same values of  $\rho_N$  and  $k_F(\Lambda)$  as in Fig. 2. The gap function falls off from its maximum at  $k(\Lambda) = 0$ , and varies very rapidly around  $k_F(\Lambda)$ . The gap function is also found to be negative over a wide range of higher momenta. As can be seen in Fig. 3, the

gap energy  $\Delta_k$  is always larger in absolute magnitude for larger nuclear matter density. This results from the enhancement of the two-particle interaction at higher background densities, as seen in Fig. 1. Since the size of the superfluid gap for a given  $k_F(\Lambda)$  is mostly dependent on the two-particle interaction at distances of about  $1/k_F(\Lambda)$ , the gap energy grows larger for a larger density of the background nuclear medium. Correspondingly, The integrand of Eq. (3) (Fig. 2) also increases for a larger  $\rho_N$ .

We note that qualitative results such as those shown in Figures 2-3 are common also in solutions of the gap equations for nucleons [7,8]. The need for a large cutoff momenta is of particular importance, since it clarifies why the gap energy estimated through the weak-coupling-approximation (WCA) [31] systematically underestimates the gap energy. In this approximation one essentially assumes that it is sufficient to integrate Eq. (3) over a narrow range near  $k_F$ . Indeed, gap energies found for nucleons through the WCA are usually lower by a factor of two and more than those derived by a self consistent solution of the gap equation (see, for example, in Ref. [7]).

The prevalent result of the solution of the gap equation is the value for the gap energy at the Fermi surface,  $\Delta_F \equiv \Delta_{k_F}$ . The resulting function  $\Delta_F(k_F)$  has a typical bell shape, ranging from  $\Delta_0 = 0$  to some maximum value and then falling off again to zero. This later part of the  $\Delta_F(k_F)$  arises from the decrease of mean inter-particle distance at higher  $k_F$ , as the  $\Lambda$ 's sample more of the repulsive core. This physical mechanism causes the S-wave superfluidity to vanish at large  $\Lambda$  partial densities. The  $\Delta_F(k_F(\Lambda))$  dependence for nuclear matter background densities equal to  $2\rho_0, 2.5\rho_0, 3\rho_0$  and  $5\rho_0$  are shown in Fig. 4. The corresponding values of the gap energies and the effective  $\Lambda$  masses for  $\rho_N = 2.5\rho_0$  and  $\rho_N = 5.0\rho_0$  are given in Table 2.

As is expected from Figs. 2-3, the gap energy for a given  $k_F(\Lambda)$  increases along with the density of the nuclear matter background,  $\rho_N$ . However, for matter composed of nucleons and  $\Lambda$ 's, increasing  $\rho_N$  alone corresponds to lowering the fraction of the  $\Lambda$ 's. On the other hand keeping the  $\Lambda$  fraction constant while increasing the total density amounts to an increase of  $\Lambda$  Fermi momenta, and it is clear from Fig. 4 that increasing  $k_F(\Lambda)$  beyond  $0.8 \text{ fm}^{-1}$  should lead to a decline in the gap energy. Thus, increasing the total baryon density with a given  $\Lambda$  fraction tends to reduce the gap energy, while a larger total baryon density also means a larger nuclear matter density, which should increase the gap energy. Hence, these two trends compete when the total baryon fraction is increased and the  $\Lambda$  fraction is kept constant.

In Fig. 5 we compare these two trends by presenting gap energies at the Fermi surface as a function of the total baryon density,  $\rho_B$ , of matter composed of nucleons and  $\Lambda$ 's. The curves represent constant  $\Lambda$  fractions of 5%, 10%, 15% and 20% of the total baryon population. As it happens for the particular pairing interaction used in this work, the two trends balance

for a  $\Lambda$  fraction of about 5%, and for a larger  $\Lambda$  fraction the gap energy decreases to zero as the total baryon density is increased. These results have direct implications on the gap energies in neutron star matter, as is discussed in the next Section.

We now return to the problem of the “true” effective masses of the baryons in dense matter. So far we have assumed that the initial mass of the  $\Lambda$  hyperons on the Fermi surface is equal to the bare mass,  $M_\Lambda = 1115.6$  MeV. Since we do not combine a self consistent treatment of bulk effects and the relativistic properties of the interactions, we must resort to arbitrary parameterization to examine the dependence of the pairing energies on the initial mass. A more accurate derivation of consistent interactions and masses is deferred to future work.

Fig. 6 demonstrates the dependence of the gap energies on the “true” effective mass of the  $\Lambda$  hyperons in the matter. The results shown are for a nuclear matter density of  $\rho_N = 2.5\rho_0$  and  $\Lambda$  initial masses taken as 0.7, 0.85 and 1.0 times the bare mass (as mentioned in Sec. II, the effective mass derived by the solution to the superfluid equations is always lower than the initial one by several percent). As is expected, a lower mass leads to higher single-particle energies for any given momenta, and this yields lower gap energies. However, the basic existence of a superfluid gap of  $\Delta_F \geq 0.1$  MeV for  $k_F(\Lambda) \leq 1.3$  fm $^{-1}$  is found also for effective masses lower than the bare mass.

A final point of interest is the the dependence of the gap energies on the matter temperature. The importance attributed to this dependence is of obvious in view of the implications of baryon superfluidity on neutron star cooling rates. We hereby follow the approach of Elgarøy et al. [8] in estimating this dependence for  $\Lambda\Lambda$ .

The gap equation at a finite temperature  $T$  is given by revising Eq. (3) to the form:

$$\Delta_k(T) = -\frac{1}{2} \frac{1}{(2\pi)^3} \int_0^\infty 4\pi k'^2 dk' V_{kk'} \frac{\Delta_{k'}(T)}{(\xi_{k'}^2(T) + \Delta_{k'}^2(T))^{\frac{1}{2}}} \tanh\left(\frac{(\xi_{k'}^2(T) + \Delta_{k'}^2(T))^{\frac{1}{2}}}{2k_B T}\right), \quad (7)$$

where  $k_B$  is the Boltzmann constant. We solve Eq. (7), while approximating the single-particle energies to be “frozen”, i.e., assuming that  $\xi_{k'}(T) = \xi_{k'}(0)$ . This should be a reasonable approximation for neutron stars, since the temperature range of interest is much lower than the Fermi energy (see [8] and references therein). We also assume that the two-particle interaction is not sensitive to the temperature in the range of interest. The gap equation is then solved in similar fashion to the zero-temperature case.

The temperature dependence of the gap energy at the Fermi surface,  $\Delta_F(T)$  for background nuclear matter density of  $\rho_N = 2.5\rho_0$  and  $\rho_N = 5\rho_0$  is shown in Fig. 7. Also shown are the critical temperatures,  $T_c$ , estimated from the WCA, given by [31]



$$k_B T_c \approx 0.57 \Delta_F(T = 0) \quad . \quad (8)$$

As in the case of nuclear matter [8], we see that the WCA does yield good agreement with the results of the full solution, provided that the value of  $\Delta_F(T = 0)$  is taken from the gap equation solution rather than the WCA for the gap, as explained above.

## V. IMPLICATIONS FOR NEUTRON STAR MATTER

Modern estimates [14-18] of hyperon formation in neutron stars agree that hyperons begin to accumulate in neutron star matter at baryon densities of about  $2\rho_0$ . In particular, the threshold baryon density for  $\Lambda$  formation is found to be about  $2.5\rho_0$ , when the chemical potential of the neutrons grows large enough to compensate for the mass difference  $M_\Lambda - M_n$ . While the fine details of the  $\Lambda$  fraction in the matter are model dependent, these basic features are widely accepted. We stress that this consensus is an immediate result of employing realistic values for the interaction of  $\Lambda$  hyperons in nuclear matter, based on experimental data of  $\Lambda$ -hypernuclei [29].

An example of the equilibrium composition of neutron star matter (assuming  $T = 0$ ) is given in Fig. 8a, based on an equation of state similar to the  $\delta = \gamma = \frac{5}{3}$  model of Ref. [18]. The steep rise in the  $\Lambda$  fraction when they first appear in the matter is common to all works that examined hyperon formation in neutron stars. This behavior is caused by the fact that lowering the nucleon fraction lowers the nucleon-nucleon repulsion and the nucleon Fermi energies, while the net interaction among the  $\Lambda$ 's is still attractive. Eventually the  $\Lambda$  fraction saturates, typically at  $0.1 - 0.2$ , and continues to grow slowly up to as much as  $0.3$  at higher densities.

Recent theoretical and experimental results of  $\Sigma^-$ -atoms suggest that the interaction of  $\Sigma$  hyperons in nuclear matter includes a strong isoscalar repulsive component [32]. If such repulsion exists, formation of  $\Sigma$  hyperons in neutron star matter is suppressed [16,18], and  $\Lambda$  production in the matter is somewhat enhanced, both by a lower threshold density and by a sharper rise of the  $\Lambda$  fraction. The main effect, though, is the formation of  $\Xi^-$  hyperons which begins at significantly lower densities (about  $3\rho_0$ ), providing the favorable negatively charged baryon fraction. The equilibrium compositions of matter without  $\Sigma$ 's is shown in Fig. 8b, using an equation of state otherwise identical to that of Fig. 8a.

In view of the absence of any experimental data on medium effects regarding different hyperon species, we assume in the following analysis that the pairing interaction discussed in Sec. 3 is valid also for a background matter which includes other species besides nucleons

(i.e.  $\Sigma$  and  $\Xi$  hyperons). For densities up to  $\sim 5\rho_0$  this is a reasonable assumption, since the non- $\Lambda$  matter is highly dominated by the nucleons. Thus, for every combination of the total baryon density and particle fractions we take  $\rho_{bg} \equiv \rho_B - \rho_\Lambda$  as the background density  $\rho_N$  for the calculation of the  $^1S_0$  gap energy.

The  $\Lambda\Lambda$  gap energies found for the baryon compositions of Figs. 8a-8b are shown in Fig. 9, as a function of the total baryon density. Also shown are the gap energies for the equilibrium composition for model PLZ of Schaffner and Mishustin [17], which predict  $\Lambda$  accumulation at slightly lower densities than the equations of [18].

As seen in Fig. 9, the qualitative behavior of the gap energies is common to all three equations of state. Pairing to a superfluid state essentially takes place once the  $\Lambda$ 's appear in the matter, and rises sharply to a maximum value following the sharp rise of the  $\Lambda$  fraction in the matter. The partial density of the non- $\Lambda$  baryons is almost constant in this range of total baryon densities. Hence, the curves approximately follows the gap energy dependence on  $k_F(\Lambda)$  for a given background density, as shown in Fig. 4. The pairing energy rises sharply as the total baryon density is increased, and then, as is expected from Fig. 5, begins to decline once the  $\Lambda$  fraction exceeds about 0.05, (note that for  $\rho_B = 2\rho_0$ ,  $k_F(\Lambda) \approx 0.8 \text{ fm}^{-1}$  is reached when the  $\Lambda$  fraction is about 5%). Since the  $\Lambda$  fraction begins to saturate at a value of 0.1–0.2, the decline of the gap energy is not as steep as in the rising part. The rate of this decline is thus somewhat model dependent, particularly whether other hyperon species (i.e. the  $\Sigma^-$ ) compete with  $\Lambda$  formation.

It should be noted that these results are qualitatively similar to those found for proton  $^1S_0$  pairing in neutron star matter, where protons are a minority among the nucleons. The density range found for a superconducting proton state lies between the threshold for free proton appearance up to densities where the proton fraction reaches about 0.1–0.2 [7,8]. However, since the proton fraction in neutron star matter is expected to rise much more moderately as a function of the total baryon density than the  $\Lambda$  fraction (see Figs. 8a-8b), the density range where a proton superconductor exists is typically larger than that found here for the  $\Lambda$  superfluid.

## VI. CONCLUSIONS AND OUTLOOK

In this work the  $^1S_0$  pairing energy of  $\Lambda$  hyperons in a nuclear matter background was evaluated using the  $G$ -Matrix effective interaction presented by Lansky and Yamamoto [25]. We find that a gap energy of a few tenths of MeV is expected for a  $\Lambda$  Fermi momenta,  $k_F(\Lambda)$ , below  $1.3 \text{ fm}^{-1}$ . The gap energy is dependent both on the  $\Lambda$  Fermi momenta and on the

density of the background nuclear matter,  $\rho_N$ . For  $\rho_N \geq 2\rho_0$  the gap energy for a given  $k_F(\Lambda)$  increases with increasing  $\rho_N$ .

Employing these results to neutron star matter with hyperons yields  $\Lambda\Lambda$   $^1S_0$  pairing for a baryon density range between the threshold density for  $\Lambda$  appearance to about the baryon density where the  $\Lambda$  fraction reaches  $\sim 0.2$ . A maximum gap energy of  $0.8-0.9$  MeV is achieved for a  $\Lambda$  fraction of about 0.05. While the exact range of densities where such pairing exists is model-dependent, the qualitative picture seems to be common to all equations of state which are based on modern evaluations of the  $\Lambda$ -nucleon interaction in nuclear matter. Gap energies in this range are larger than the temperature predicted in neutron star cores, and thus imply that a  $\Lambda$   $^1S_0$  superfluid will exist in the core, typically within a baryon density range of  $\rho_B \approx 2-3\rho_0$ .

We comment that the present results must be treated as a preliminary evaluation of  $\Lambda$  pairing in dense matter. The evaluation of the two-particle interaction is based on hypernuclei experiments, where the nuclear matter density is limited to  $\rho_N \approx \rho_0$ , so that the effective interaction might not be as good an approximation as in the case of neutron pairing. In particular, the present work does not include relativistic corrections which might be significant at the baryon densities where hyperons form in neutron star matter (note however, that relativistic corrections for proton  $^1S_0$  pairing at about the same densities have been found to introduce only small corrections to the nonrelativistic results [33]). It is also noteworthy that we have not included particle-hole correlations which have been shown to be important in the evaluation of gap energies [6]. In short, further work is necessary to produce more realistic results, preferably with a better founded  $\Lambda$ - $\Lambda$  interaction in a high density nuclear matter background.

We believe that formal treatment of the non-nucleon component in the background neutron star matter, will not significantly effect the results found here. This is especially true if  $\Sigma$  hyperon formation is suppressed, so that the baryon equilibrium compositions include only nucleons and  $\Lambda$ 's throughout the entire range where pairing is expected. Nonetheless, taking other hyperon species into account is clearly desirable in a more rigorous model. Obviously, hyperon-hyperon interactions in a dense matter background will also provide a basis for estimation of possible pairing of other hyperon species in neutron stars. For example,  $\Sigma^-$  pairing is of special interest, since the  $\Sigma^-$  is also expected to appear at relatively low baryon densities in neutron stars (if  $\Sigma$  formation is not suppressed). However, no relevant experimental data is currently available. The commonly assumed universal hyperon-hyperon interaction implies that the  $\Lambda\Lambda$  gaps may serve as indication for  $\Sigma$  and  $\Xi$  pairing in dense matter. More accurate results require, however, the inclusion of isospin-dependent forces, which are absent in the  $\Lambda$  case.

The large majority of dense matter equations of state require neutron star central densities larger than the threshold density for  $\Lambda$  formation, i.e. baryon densities larger than  $\sim 2.5\rho_0$ . Hence, it is likely that neutron stars do include a region where the  $\Lambda$ 's pair to a  $^1S_0$  superfluid. Whether or not the central density of a neutron star exceeds the density range for  $^1S_0$   $\Lambda\Lambda$  pairing depends on its mass and on the actual equation of state. Note, however, that at larger densities higher order pairing may also be available, including inter-species pairing [10]. In fact,  $\Lambda n$  pairing may be more likely than  $pn$  pairing, since at baryon densities of  $\rho_B \gtrsim 4\rho_0$  the  $\Lambda$  and neutron fractions are expected to be comparable.

Finally, we recall that the existence of a  $^1S_0$   $\Lambda$  superfluid for baryon densities relevant to neutron stars implies significant suppression of  $\Lambda$ -direct Urca cooling. The onset of superfluidity reduces the neutrino emissivity, along with the heat capacity and thermal conductivity, by a factor of  $\exp(-\Delta_F/k_B T)$ . In view of our results here, we suggest that implications of hyperon superfluidity on neutron star cooling rates are well worth examination.

#### ACKNOWLEDGMENTS

We are grateful to Avraham Gal for valuable discussions and comments. We also thank Jürgen Schaffner for providing us with equilibrium compositions of the relativistic mean field calculations. One of us (S.B.) also thanks Meir Weger for helpful guidance regarding the BCS theory. This research was partially supported by the U.S.-Israel Binational Science Foundation grant 94-68.

## References

---

- [1] A.B. Migdal, Sov. Phys. JETP **10**, 176 (1960).
- [2] T. Takatsuka, Prog. Theo. Phys. **48**, 1517 (1972).
- [3] M. Hoffberg, A. E. Glassgold, R. W. Richardson and M Ruderman, Phys. Rev. Lett. **24**, 775 (1970).
- [4] L. Amundsen and E. Ostegaard, Nucl. Phys. **A437**, 487 (1985)
- [5] M. Baldo, J. Cugnon, A. Lejeune and U. Lombardo, Nucl. Phys. **A515**, 409 (1990).
- [6] J. Wambach, T. L. Ainsworth and D. Pines, Nucl. Phys. **A555**, 128 (1993).
- [7] J. M. C. Chen, J. W. Clark, R. D. Davé and V. V. Khodel, Nucl. Phys. **A555**, 59 (1993).
- [8] O. Elgarøy, L. Engvik, M. Hjorth-Jensen, and E. Osnes, Nucl. Phys. **A604**, 466 (1996).
- [9] O. Elgarøy, L. Engvik, M. Hjorth-Jensen and E. Osnes, Nucl. Phys. **A607**, 425 (1996), and references therein.
- [10] T. Takatsuka and R. Tamagaki Prog. Theo. Phys. Suppl., **112**, 27 (1993).
- [11] D. Pines and M. A. Alpar, Nature **316**, 27 (1985). M. A. Alpar, H. F. Chau, K. S. Cheng and D. Pines, Astrophys. J. **409**, 345 (1993).
- [12] C. Schaab, D. Voskresensky, A. D. Sedrakian, F. Weber, and M.K. Weigel, Astron. Astrophys. **321**, 591 (1997).
- [13] J. M. Lattimer, K. A. Van Riper, M. Prakash and M. Prakash, Astrophys. J. **425**, 802 (1994).
- [14] N.K. Glendenning, Astrophys. J. **293**, 470 (1985).
- [15] F. Weber and M. K. Weigel, Nucl. Phys. **A505**, 779 (1989).
- [16] R. Knorren, M. Prakash and P.J. Ellis, Phys. Rev. C **52**, 3470 (1995).
- [17] J. Schaffner and I.N. Mishustin, Phys. Rev. C **53**, 1416 (1996).
- [18] S. Balberg and A. Gal, Nucl. Phys. **A** (in press, 1997). LANL preprint archive index nucl-th/9704013.
- [19] C. Schaab, F. Weber, M.K. Wiegel and N.K. Glendenning, Nucl. Phys. **A605**, 531 (1996).

- [20] M. Prakash, M. Prakash, J.M. Lattimer and C.J. Pethick, *Astrophys. J.* **390**, L77 (1992).
- [21] M. Prakash, *Phys. Rep.* **242**, 297 (1994).
- [22] P. Haensel and O. Yu. Gnedin, *Astron. Astrophys.* **290**, 458 (1994).
- [23] H. Umeda, S. Tsuruta and K. Nomoto, *Astrophys. J.* **433**, 256 (1994).
- [24] S. Aoki et al., *Prog. Theor. Phys.* **85**, 1287 (1991). K. Imai, *Nucl. Phys.* **A547**, 653 (1992).
- [25] D. E. Lansky and Y. Yamamoto, *Phys. Rev. C* **55**, 2330 (1997).
- [26] J. Bardeen, L. N. Cooper and J. R. Schrieffer, *Phys. Rev.* **108**, 1175 (1957).
- [27] A. deShalit and H. Feshbach, *Theoretical Nuclear Physics, Vol. 1: Nuclear Structure* (Wiley, New York, 1974), chapter VII.
- [28] M. Barranco and J. Treiner, *Nucl. Phys.* **A351**, 269 (1981).
- [29] For a review of hypernuclei experiments, see R.E. Chrien and C.B. Dover, *Ann. Rev. Nuc. Part. Sci.* **39**, 227 (1989).
- [30] A.R. Bodmer and Q.N. Usmani, *Nucl. Phys.* **A468**, 653 (1987).
- [31] E. M. Lifshitz and L. P. Pitaevskii, *Statistical Physics, part 2* (Pergamon, Oxford, 1980), pgs. 152-158.
- [32] C.J. Batty, E. Friedman and A. Gal, *Phys. Lett.* **335**, 273 (1994). J. Mares, E. Friedman, A. Gal and B.K. Jennings, *Nucl. Phys.* **A594**, 311 (1995).
- [33] O. Elgaroy, L. Engvik, M. Hjorth-Jensen, and E. Osnes, *Phys. Rev. Lett.* **77**, 1428 (1996).

## Figure Captions

Figure 1: The radial dependence derived for the  $\Lambda\Lambda$   $G$ -matrix interaction presented in [25]. The curves correspond to nuclear matter background densities of  $\rho_N = \rho_0$ ,  $2.5\rho_0$  and  $5\rho_0$ , where  $\rho_0$  is the nuclear saturation density.

Figure 2: The integrand of the gap equation, Eq. (3), for  $k_F(\Lambda) = 1 \text{ fm}^{-1}$ , as a function of the secondary momenta  $k'$ . The curves correspond to nuclear matter background densities of  $\rho_N = 2.5\rho_0$  and  $5\rho_0$ .

Figure 3: The gap function,  $\Delta_k$ , when  $k_F(\Lambda) = 1 \text{ fm}^{-1}$  and nuclear matter background densities of  $\rho_N = 2.5\rho_0$  and  $5\rho_0$ .

Figure 4: The gap energy  $\Delta_F$  for  $\Lambda\Lambda$  pairing as a function of the Fermi momenta, for nuclear matter background densities of  $\rho_N = 2\rho_0$ ,  $2.5\rho_0$ ,  $3\rho_0$  and  $5\rho_0$ .

Figure 5: The gap energy for  $\Lambda\Lambda$  pairing as a function of the total baryon density,  $\rho_B$ , for different fixed  $\Lambda$  fractions.

Figure 6: The gap energy  $\Delta_F$  for  $\Lambda\Lambda$  pairing as a function of the Fermi momenta, for different values of the initial mass of  $\Lambda$  hyperons in the matter. The nuclear matter background density is taken as  $\rho_N = 2.5\rho_0$ .

Figure 7: Temperature dependence of the gap energy for  $k_F(\Lambda) = 1 \text{ fm}^{-1}$  for nuclear matter background densities of  $\rho_N = 2.5\rho_0$  and  $5\rho_0$ . Also indicated are the corresponding weak-coupling estimates for the critical temperatures.

Figure 8a: The equilibrium compositions of neutron star matter with hyperons, as a function of the total baryon density,  $\rho_B$ . The compositions were calculated with an equation of state similar to the  $\delta = \gamma = \frac{5}{3}$  model from [18].

Figure 8b: Same as Fig. 8a, but when  $\Sigma$  hyperons are repelled by the nucleons and their formation is thus suppressed.

Figure 9: The gap energy of  $\Lambda\Lambda$   $^1S_0$  pairing in neutron star matter as a function of the total baryon density. The equilibrium compositions of the matter are those of Figs. 8a (BG+ $\Sigma$ ) and 8b (BG- $\Sigma$ ), and for model PLZ of Schaffner and Mishustin [17] ( $SM_{PLZ}$ ).

TABLE I.

Parameters of the  ${}^1S_0$  state of the  $\Lambda\Lambda$   $G$ -matrix potential (model ND of [25])

$\beta_i$ (fm)	$a_i$ (MeV)	$b_i$ (MeV fm)	$c_i$ (MeV fm <sup>2</sup> )
0.5	835.5	-252.7	122.7
0.9	-298.5	156.6	-55.07
1.5	-10.80	3.0398	-1.126

TABLE II.

 $\Lambda\Lambda$   ${}^1S_0$  pairing energy gaps and effective masses

$k_F(\Lambda)$ (fm <sup>-1</sup> )	$\rho_N = 2.5\rho_0$		$\rho_N = 5\rho_0$	
	$M^*/M$	$\Delta_F$ (MeV)	$M^*/M$	$\Delta_F$ (MeV)
0.2	0.9967	0.0432	0.9963	0.1321
0.3	0.9895	0.1767	0.9881	0.3897
0.4	0.9771	0.3749	0.9740	0.7143
0.5	0.9596	0.5868	0.9543	1.0371
0.6	0.9383	0.7628	0.9304	1.2998
0.7	0.9150	0.8677	0.9042	1.4611
0.8	0.8915	0.8735	0.8779	1.4937
0.9	0.8693	0.7826	0.8532	1.3876
1.0	0.8497	0.6130	0.8313	1.1574
1.1	0.8335	0.4027	0.8132	0.8409
1.2	0.8211	0.2053	0.7993	0.5262
1.3	0.8128	0.0495	0.7900	0.1810



figure 1

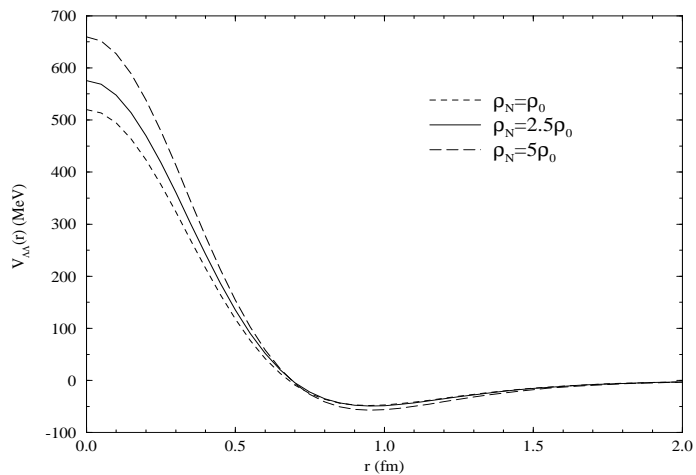


figure 2

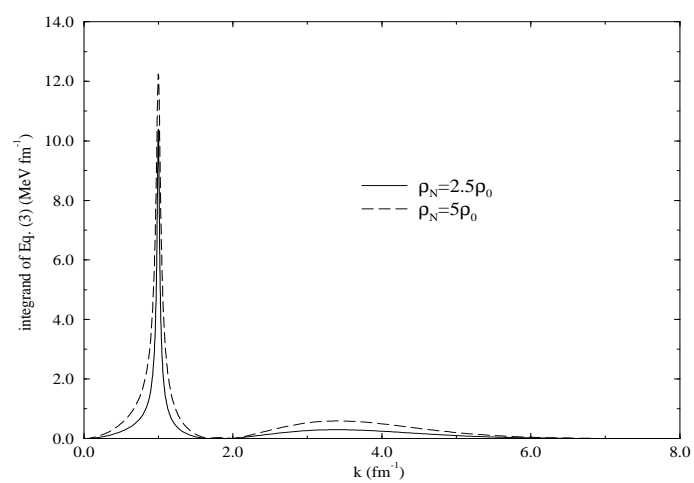


figure 3

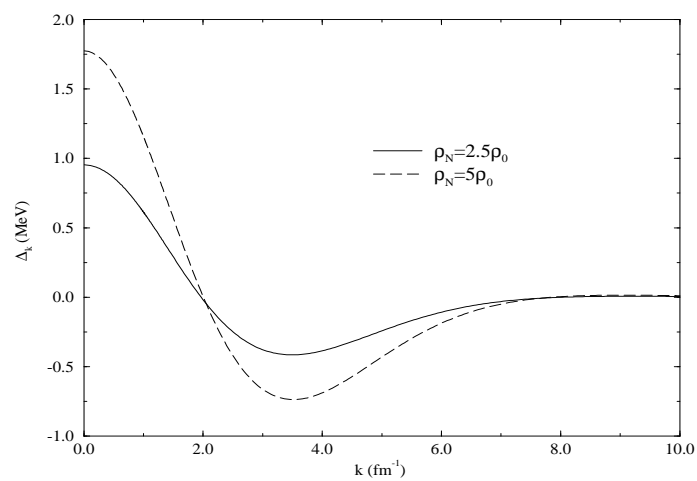


figure 4

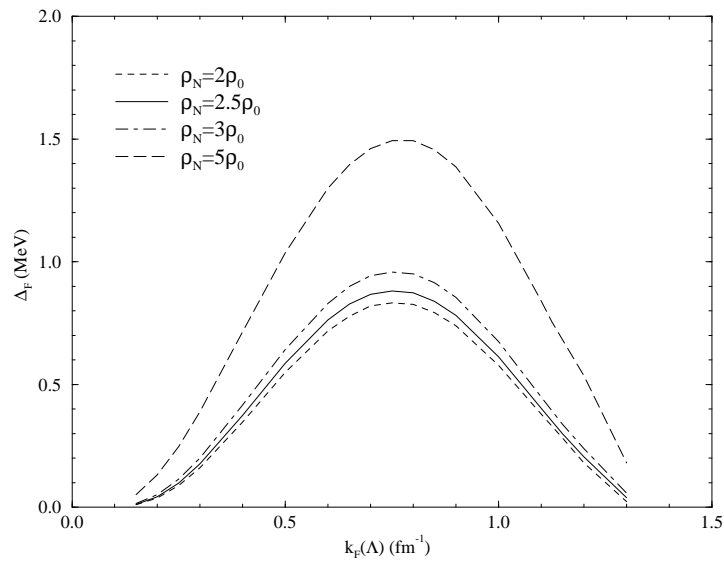


figure 5

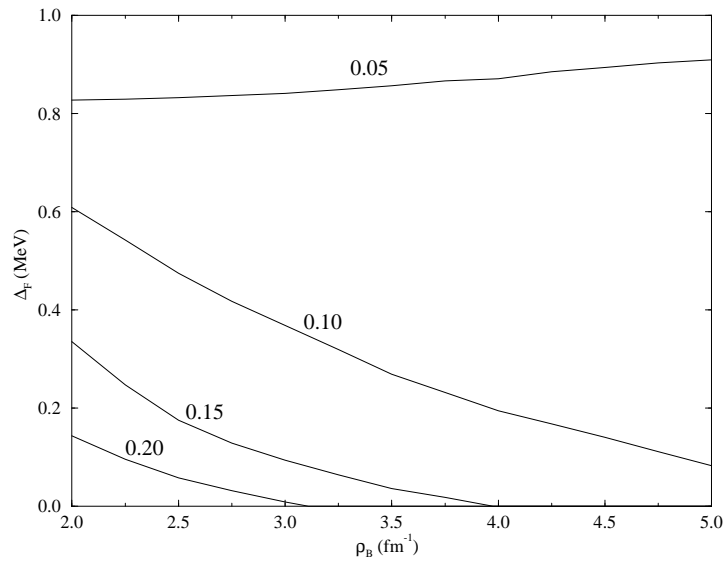


figure 6

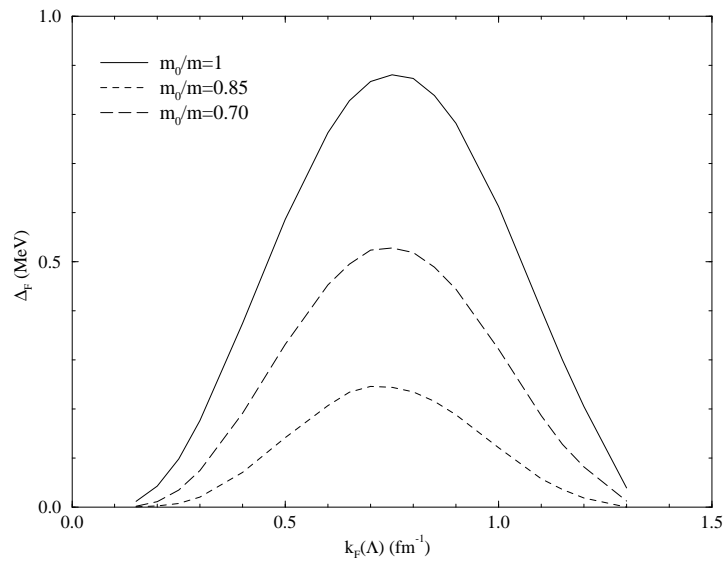


figure 7

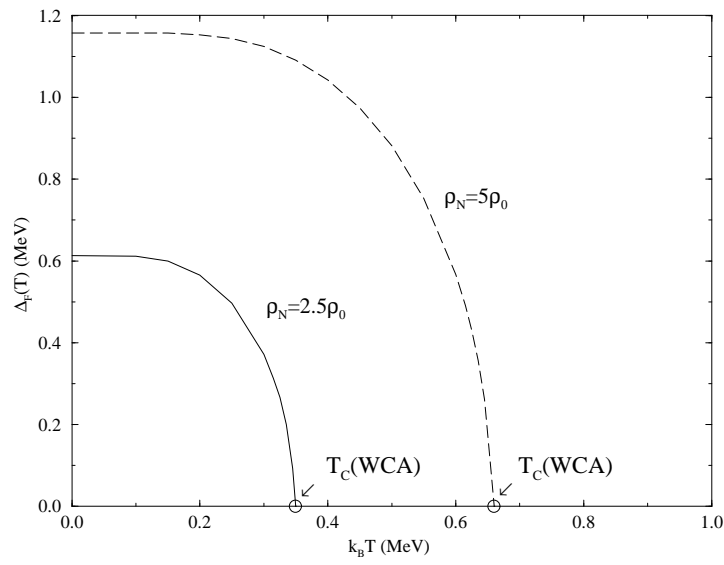


figure 8

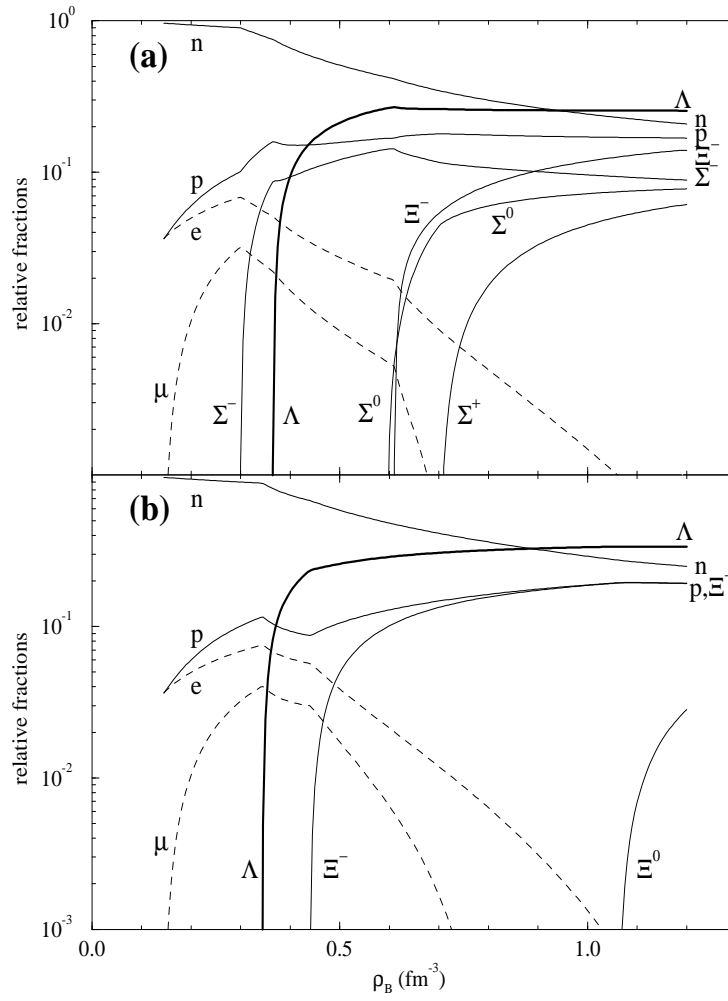


figure 9

